Desalination and Water Treatment
www.deswater.com

doi: 10.5004/dwt.2019.23271

139 (2019) 7–13
January

Mechanism of scaling on reservoir formation damage by polymer-containing wastewater re-injection

Yi-gang Liu[a], Hua-xing Chen[a], Hong-ming Tang[b,*], Yu-tian Feng[a], Ming Pang[a]

[a]*CNOOC (China) CO., Ltd., Tianjin Branch, Tianjin 300452, China, email: 307048122@qq.com (Y.-G. Liu), chenhuaxing88@163.com (H.-X. Chen), fengyt6@cnooc.com.cn (Y.-T. Feng), pangming3@cnooc.com.cn (M. Pang)*
[b]*School of Geoscience and Technology, Southwest Petroleum University, Chengdu 610500, Sichuan Province, China, email: hongmtang@126.com (H.-M. Tang)*

Received 9 March 2018; Accepted 11 October 2018

ABSTRACT

The water quality of oilfield produced water from polymer flooding (PWPF) is one of the most pressing issues in polymer-flooded oilfields. In this study, Suizhong 36-1 oilfield in the Bohai Sea was taken as the research objective, the influence and mechanism of polymer on scaling were investigated through compatibility experiment. Scanning electron microscopy and nuclear magnetic resonance spectroscopy techniques were used to analyze the effect of PWPF scaling on pore throat structures of reservoir cores. The results show that the main composition of scale was calcium carbonate, and the output polymer could enhance the incompatibility of PWPF and formation water. PWPF exhibited higher reservoir damage than source water. Amorphous scale substances were adsorbed onto mineral surface and filled inter granular pores, resulting in plugging of macro pores and mesopores.

Keywords: Polymer-containing wastewater; Wastewater reinjection; Scaling mechanism; Pore throat structure

1. Introduction

Polymer flooding is an effective method to enhance oil recovery for middle/high water-cut oilfields [1]. The polymer flooding technique has been applied in offshore oilfields of China National Offshore Oil Corporation (CNOOC) since 2003 [2].

Due to the limited space, special environmental requirement and timeliness, the mixture of source water (from water source wells) and production wastewater is extensively used as injection water for oil displacement and pressure maintenance in offshore oilfields [3]. Oilfield produced water from polymer flooding (PWPF) is characterized by high levels of viscosity, oily content, and suspended solids (SS) concentration, because of high residual polyacrylamide (PAM) content [4]. This causes a great difficulty in treating PWPF relative to the wastewater from water flooding, because the polymer can tightly bound with the oil and water and its electrostatic/steric effects can stabilize oil–water emulsions. Thus, the quality of PWPF in offshore oilfields after treatment can not meet the standard of injection water because of the limitation of wastewater treatment apparatus and technologies used in offshore platforms [5]. However, this treated PWPF was still re-injected into the reservoir formation because of the deficiency of sufficient source water and the stringent discharge standard.

One perceived problem associated with re-injection of PWPF in the field is a potential decrease in injectivity caused by formation damage by the adsorption/retention, clogging and scaling of polymers [6]. Formation damage means reducing formation permeability, leading to decreased production and injection rates [7]. The adsorption of polymer molecules to the formation grains may cause a local buildup of polymer concentration at pore throats, which in turn leads to a reduction in the permeability [8]. More-

*Corresponding author.

over, the flowing pressure will drop below the bubble point pressure or dew point pressure, resulting in the release of dissolved gas or liquid condensate dropout. If the injection rate is maintained for an injection well with formation damage, the injection pressure would be too high so that the formation could be fractured [7].

Studies have shown that the adsorption of polymer molecules to the formation grains results in a local buildup of polymer concentration at pore throats, which in turn causes a reduction in the pem1eability. It is usually difficult to remove polymer induced formation damage [9]. However, there are few studies of scaling mechanism of polymer-containing wastewater. Therefore, this work focuses on investigating the influence and mechanism of polymer on scaling, and the influence of scale on reservoir seepage characteristics and pore-throat structure.

2. Materials and methods

2.1. Materials

PWPF was collected from Bohai Basin, China. This wastewater has been treated by air flotation/demulsification in the offshore platform. Source water was obtained from Well A3W without chemical dosing. The characteristics of PWPF and source water are listed in Table 1. On the basis of field operation, PWPF and source water were mixed at a 3:1 ratio (v/v) to produce injection water. Formation water was originated from Well M5 in the Bohai Basin, China. A hydrophobic graft polymer (AP-P4, Fig. 1) with an average molecular weight of 1.0×10^7 g/mol was produced by Sichuan Guangya Polymer Chemical Co., Ltd., China. A commercial scale inhibitor (BHF-08) was provided by Tianjin Branch Company, CNOOC.

2.2. Compatibility experiment

The compatibility experiment was conducted as follows:

1. 250 mL-Erlenmeyer flasks were washed, dried and weighed for use. Glass slides were placed into the flasks in order to facilitate observation and analysis of the scale after settlement.
2. The Ca^{2+} concentration of source water, PWPF and formation water was determined by an X-ray fluorescence spectrometer (Axios Pw4400, Panalytical BV Co., Netherlands).
3. Injection water and formation water were well mixed at various volume ratios (1:0, 5:1, 3:1, 2:1, 1:1, 1:2, 1:3, 1:5, 1:7 and 0:1, total volume 200 mL) in a flask, sealed and allowed to settle for 8 h at 65°C.
4. Before and after experiments, injection water, formation water, and their mixture (after 8 h settlement) were filtered through 0.45-μm filters. The sum volume of injection water and formation water is 200 mL. According to the requirements of the SY/T 5329-2012 standard (a criterion of China Petroleum Industry), the content of suspended scale in water was calculated as follows:

$$C_{suspended} = \frac{m_m - m_i - m_f}{V} \quad (1)$$

where $C_{suspended}$ is the content of suspended scale (mg/L), m_m is the dry weight (mg) of filter after filtration with the mixture of injection water and formation water, m_i the dry weight (mg) of filter after filtration with injection water, m_f the dry weight (mg) of filter after filtration with formation water, V the total volume (liter) of the mixture of injection water and formation water.
5. After water filtration, the flasks were dried, cooled, and weighed. The content of settled scale was calculated as follows:

$$C_{settled} = \frac{m - m_0}{V} \quad (2)$$

where $C_{settled}$ is the content of settled scale (mg/L), m the dry weight (mg) of clean flasks before experiments, m_0 the dry weight (mg) of flasks after filtration, V the total volume (liter) of the mixture of injection water and formation water.
6. The content of total scale was calculated as follows:

$$C = C_{suspended} + C_{settled} \quad (3)$$

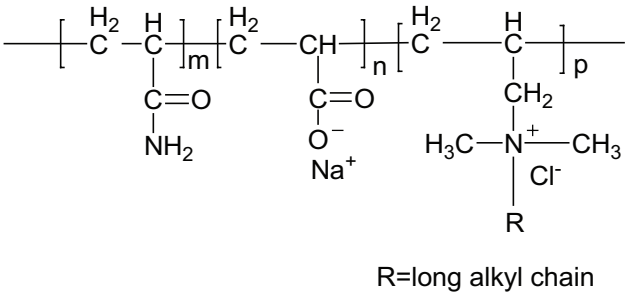

Fig. 1. The structural formulas of AP-P4 used in this study.

Table 1
The characteristics of PWPF and source water

Sample	pH	Concentration (mg/L)						Mineralization (mg/L)
		K^++Na^+	Ca^{2+}	Mg^{2+}	Cl^-	SO_4^{2-}	HCO_3^-	
PWPF	7.7	2330	343	116	4520	13	445	7767
Source water	7.5	2597	743	311	5980	73	210	9914

2.3. Core dynamic damage assessment

1. According to the analysis result of formation water, a KCl solution with the same salinity as in formation water was prepared with distilled water and KCl, for a purpose to avoid scaling of injection water and formation water.
2. The reservoir core was dried at 105°C, and weighed, and gas permeability (K_g) of the core was determined.
3. The core was evacuated, saturated with KCl solution for at least 24 h, placed in a Hassler core holder, and maintained at 65°C. The core was then flooded with KCl solution at a flow rate of 1 mL/min, and the initial core permeability (K_i) was determined.
4. The core was then flooded with at least 80 PV of different injection water/formation water mixtures at a rate of 1 mL/min.
5. Finally, the core was flooded with at least 80 PV of KCl solution (1 mL/min), and the recovered permeability (K_r) was determined.
6. The damage extent of core permeability was calculated as follows:

$$I = (1 - K_r / K_i) \times 100\% \quad (4)$$

where I is the damage extent of core permeability, K_i the initial core permeability, K_r the recovered permeability.

2.4. Instrumental analysis

Scanning electron microscopy (SEM) was conducted with a FEI Quanta 450 field emission scanning and an Edax Octane energy-dispersive X-ray (EDS) system with a 60 mm² detector. Pore structure characteristics of core samples were investigated by using nuclear magnetic resonance (NMR) spectroscopy (model MacoMR12-150H-1, Shanghai Niumai Electronic Technology Co., Ltd., China), following the method of Liu et al. [10].

3. Results and discussion

3.1. Effect of output polymer concentration on scale content

Whether it is polymer-containing wastewater or conventional wastewater, the composition of scale substances produced by mixing with the wastewater and source water is mainly $CaCO_3$ particles with different amounts, morphologies and sizes. To study the influence of output polymer from PWPF on the growth of scale, compatibility experiments were conducted using the mixture of injection water and formation water at various volume ratios. The yield, morphology and composition of scale were analyzed. The effect of polymer concentration on scale morphology was also studied based on the growth mechanism of calcium carbonate minerals.

In this work, the total content of scale (C) was calculated according to the above-mentioned equations [Eqs.(1)–(3)]. Additionally, a theoretical scale content (C') was defined as follows:

$$C' = \frac{m}{m+n} \times C_i + \frac{n}{m+n} \times C_f \quad (5)$$

where C' is the theoretical scale content, C_i the measured value of scale content with injection water alone, C_f the measured value of scale content with formation water alone, m/n the volume ratio of injection water to formation water.

As shown in Fig. 2, total scale content (C), theoretical scale content (C'), and scale increment (C–C') generally increases as polymer concentration is increased with some fluctuations. This result demonstrates that output polymer could promote scaling and enhance the incompatibility of injection water and formation water.

3.2. Effect of output polymer on scale morphology

Fig. 3 shows the SEM micrographs of suspended scale and settled scale formed under different concentrations of output polymer, and the corresponding EDS analysis results of the red box-boundary regions are listed in Table 2.

The particles of suspended scale had a flat rhombohedral shape with clear edge and a particle size of 50 μm in the absence of polymer (Fig. 3a). When polymer was present, the suspended scale particles accumulated together as sheet, film, or cloddy shapes, and the particles were wrapped by membranous substances (Figs. 3b,c).

The particles of settled scale formed rhombohedral crystals with a size of 50 μm in the absence of polymer (Fig. 3d). These particles shrunk to spherical particle with an average size of 3 μm in the presence of polymer (Figs. 3e, f). Additionally, there existed a thin polymer film underneath the particles (Figs. 3e, f).

The EDS analysis results demonstrate that the main element composition of scale particles was C, O and Ca, which accounted for more than 90% of total mass. Thus, it can be inferred that the scale particles demonstrated by SEM (Fig. 3) were $CaCO_3$ particles.

The above-mentioned results demonstrate that, the influence of output polymer on scale content during compatibility experiment was intensified with the increase of

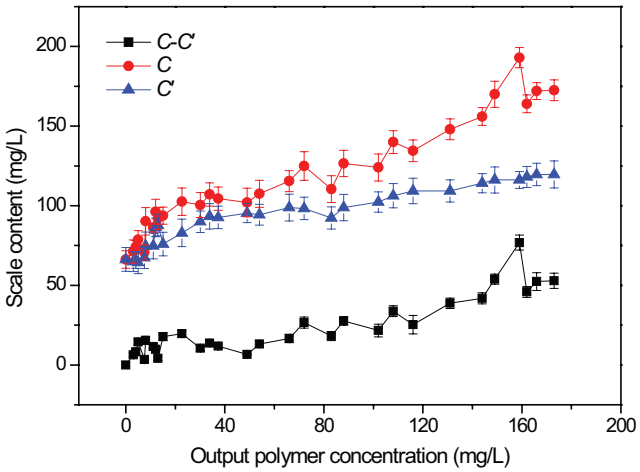

Fig. 2. Effect of output polymer concentration on scale content. C, total scale content; C', theoretical scale content; C-C', scale increment.

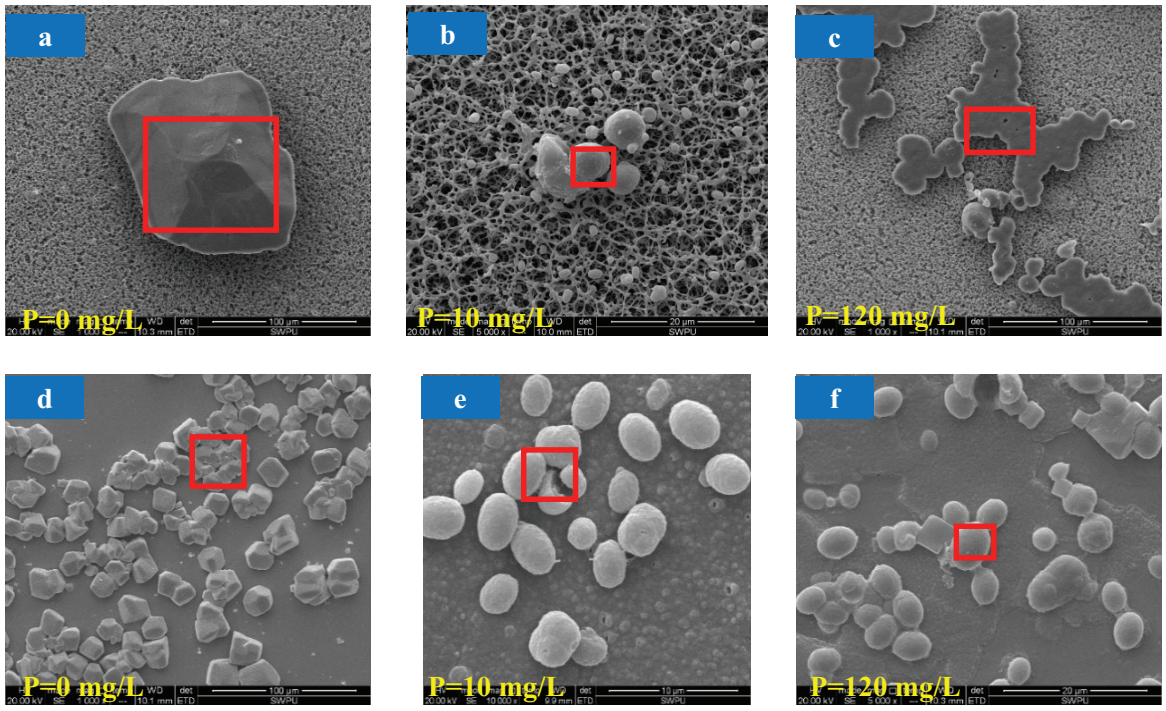

Fig. 3. SEM micrographs of suspended scale (a, b and c) and settled scale (d, e and f) formed under different concentrations of output polymer. P: polymer concentration. The region of red rectangles is specified for EDS analysis.

Table 2
The results of EDS analysis of suspended scale (a, b and c) and settled scale (d, e and f)

Sample	Polymer concentration (mg/L)	Mass%				
		C	O	Ca	Si	Mg
a	0	23.23	37.17	37.25	1.31	1.04
b	10	24.95	30.96	44.08	–	–
c	120	26.8	33.57	39.63	–	–
d	0	27.83	32.18	38.76	–	1.23
e	10	34.95	44.08	20.97	–	–
f	120	35.77	30.71	25.82	3.14	4.56

polymer concentration (Fig. 2), whereas polymer had little effect on scale composition (Table 2). However, the morphology of scale was affected significantly by polymer (Fig. 3), namely the presence of polymer could greatly reduce scale particle size, leading to the migration of scale particles to deep reservoirs. Moreover, these $CaCO_3$ microspheres could aggregate into larger particles with sheet, film or cloddy shapes (Fig. 3), which may cause blocks in the zone close to oil wells.

3.3. Regulation mechanism of output polymer in the morphology and crystal types of scale

Generally speaking, the crystallization of a solute out of solution usually undergoes two steps: firstly, tiny particles are formed as crystalline cores (namely crystal nuclei); subsequently, crystal nuclei grow into visible crystal particles. The process of crystalline formation is called nucleation, and the crystalline nuclei then grow into microcrystalline particles. Microcrystalline particles in solution collide with each other and grow up due to the Brownian movement of the particles. Such a process is called crystal growth. The precipitation process of calcium carbonate crystals consists of crystalline nucleus formation, nucleus growth, crystalline-state transformation, and the stability period of crystal number and size [11,12].

According to the classic crystal nucleation theory [13], the nucleation process can be promoted by lowering surface free-energy barrier or increasing solution saturation; if the net crystalline-substrate inter facial free-energy is lower than that of crystalline-solution, heterogeneous nucleation would occur preferentially. On the basis of the study on shell nacre, Weiner and Addadi [14] pointed out that, activation energy of inorganic heterogeneous nucleation could be reduced when the periodic structure of organic matrix is adapted to the periodic lattice constant of crystal network in a certain direction. This may induce oriented growth of polyacrylamide (PAM) crystals along the crystal network in this direction, thereby enabling the crystal axis of the network perpendicular to the template plane (Fig. 4).

PAM is the most widely used polymer for oilfield polymer flooding practice. The formation of flat rhombohedrical crystals (Figs. 3a, d) is due to the influence of PAM on some growing crystal faces through selective adsorption of the polymer chains forcing the crystal to grow in two dimensions [13,14]. The resulting platelets then aggregated to form polycrystals in order to lower their interface energy. The functional groups such as C=O, and >N–H were sug-

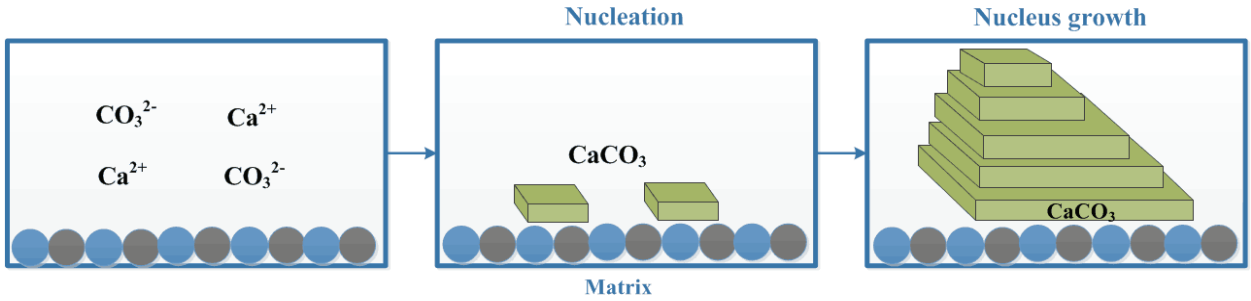

Fig. 4. Schematic illustration of the thermodynamic process of $CaCO_3$ crystal formation.

Table 3
An adaptive dynamic evaluation of reservoir cores collected from Suizhong 36-1 oilfield

Core number	Sampling depth of cores (m)	Injected water	K_g (md)	K_i (md)	K_r (md)	KCl solution salinity (mg/L)	I (%)	Core damage
1	1593	Source water	3314	292	166	8000	43.03	Moderately weak
2	1679		1539	172	79	8000	54.31	Moderately strong
3	1618	Source water dosed with 30 mg/L scale inhibitor	2989	122	112	8000	11.96	Weak
4	1642		3730	259	228	8000	8.37	Weak
5	1380	PWPF	3539	461	233	8000	49.46	Moderately weak
6	1504		2292	193	86	8000	55.44	Moderately strong

Note: K_g, gas permeability; K_i, initial core permeability; K_r, recovered permeability; I, damage extent of core permeability.

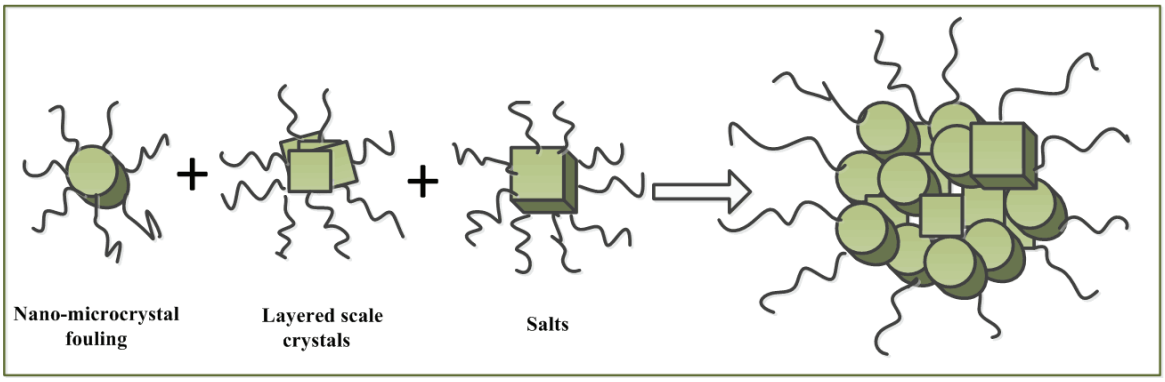

Fig. 5. The diagram of polymer, crystal and salt crosslinking.

gested to affect the nucleation and growth of $CaCO_3$ crystals [15]. A consideration of the polarity of the –N–C bond in PAM molecule, in which the negative charge is shifted towards the oxygen atom, suggesting that the formation of $CaCO_3$ crystals may be initiated through the interaction of Ca^{2+} ions with the end of the C=O bond.

The crystals obtained in the presence of polymer (namely PAM) were mono-dispersed spherical crystals (Figs. 3e, f). The surface of the rhombohedra crystals has concaves and this may be due to dissolution of $CaCO_3$, which then re-crystallized to form secondary crystals [16] on the surface of the crystals as observed in Figs. 3e, f. This phenomenon has been reported by Wang et al. [17], who suggested that the less thermodynamically stable polymorphs can dissolve from the surface of the crystals. Dissolution of $CaCO_3$ from the surface may then be followed by re-crystallization, forming a more thermodynamic stable polymorph. Secondary crystallization can also result in a mixture of crystal morphologies and generally smaller crystals compared to the primary crystals were observed [18]. In reservoirs, nano-microcrystal fouling, layered scale crystals and salts can be cross linked to form a larger-sized complex (Fig. 5), resulting in blockage of reservoir gap [17,18].

3.4. Effect of PWPF on reservoir permeability

Table 3 lists the adaptive dynamic evaluation of reservoir cores flooded with various solutions during core dynamic damage experiments. According to the damage extent of core permeability, core damage was classified into four classes: weak ($I < 30$), moderately weak ($30 \leqslant I \leqslant 50$),

moderately strong ($50 \leqslant I < 70$), and strong ($70 \leqslant I$) [7]. Source water flooding exhibited moderately weak-moderately strong core damage, and this damage could be greatly lessened by scale inhibitor addition (Table 3). PWPF flooding showed higher core damage than that of source water, indicating that the scale formed through re-injection of polymer-containing wastewater could aggravate reservoir damage.

3.5. Effect of PWPF on pore throat structure

During oilfield production, reservoir scaling would be increased when formation water is injected into the reservoir along with incompatible water for a long time. This may cause blocks in the zone close to oil wells, leading to increased water injection pressure and frequent oil well acidification. In this work, SEM and NMR techniques were applied to investigating the influence of scaling on reservoir pore throat structure.

There existed a large amount of amorphous substances which were adsorbed onto mineral surface and filled intergranular pores (Fig. 6a). Some membranous substances were attached onto the surface of skeleton particles and clay minerals, and the surface of membranous substances was covered with many globular scale particles with various sizes (Fig. 6b). The membranous substances were homogeneous and dense, and no apparent pores and seams were observed (Fig. 6c). These membranous substances could be clogged in the pore throat, resulting in plugging of the subsequent fluid and thus core permeability damage.

Secondary crystallization can also result in a mixture of crystal morphologies and generally smaller crystals compared to the primary crystals were observed [17]. In reservoirs, nano-microcrystal fouling, layered scale crystals and salts can be cross linked to form a larger-sized complex (Fig. 5), resulting in blockage of reservoir gap.

NMR is a non-destructive, quantitative and refined method for characterizing pore structure. NMR can detect the relaxation characteristics of hydrogen nuclei in fluids under external magnetic field and reflect the pore throat distribution [19]. Fig. 7 shows the pore structure change of core samples (corresponding to cores in Table 3) suggested by NMR before and after displacement experiments. As far as no.2 core is concerned, after displacement test with source water, the proportion of macro pores significantly decreased, whereas the proportion of mesopores slightly declined (Fig. 7). Although some native small pore throats were clogged with scale during experiments, large pore throats were filled by regular crystalline scale of source water and divided into some small pore throats. Thus, the number of small pore throats (indicated by the proportion of mesopores) decreased slightly after test. As for no. 6 core, after displacement test with PWPF, the proportions of both macro pores and mesopores significantly decreased, whereas the proportion of small pores changed slightly (Fig. 7). This demonstrates that macro pores and mesopores could be severely plugged with the scale complex.

4. Conclusions

The results of the present study demonstrate that the re-injection of PWPF into reservoirs could enhance reservoir permeability damage. Polymer in PWPF could not only exacerbate incompatibility of injection water, but also reduce scale particle size. Because of polymer adsorption effect, nano-microcrystal fouling, layered scale crystals and salts can be cross linked to form a larger-sized complex, leading to blockage of reservoir gap. Scale formed by PWPF injection produced greater reservoir damage than that by source water.

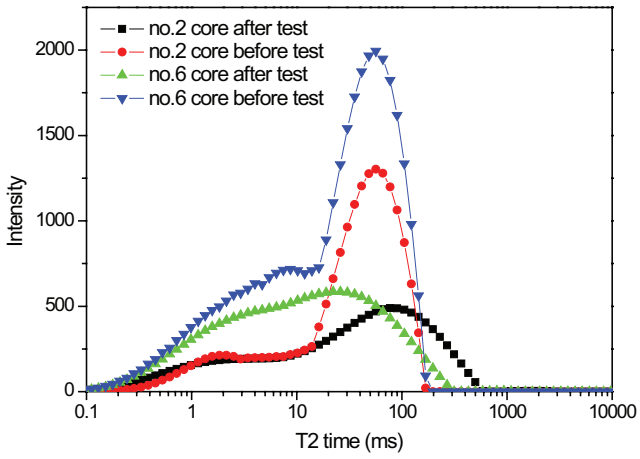

Fig. 7. Pore structure change of core samples suggested by NMR before and after displacement test.

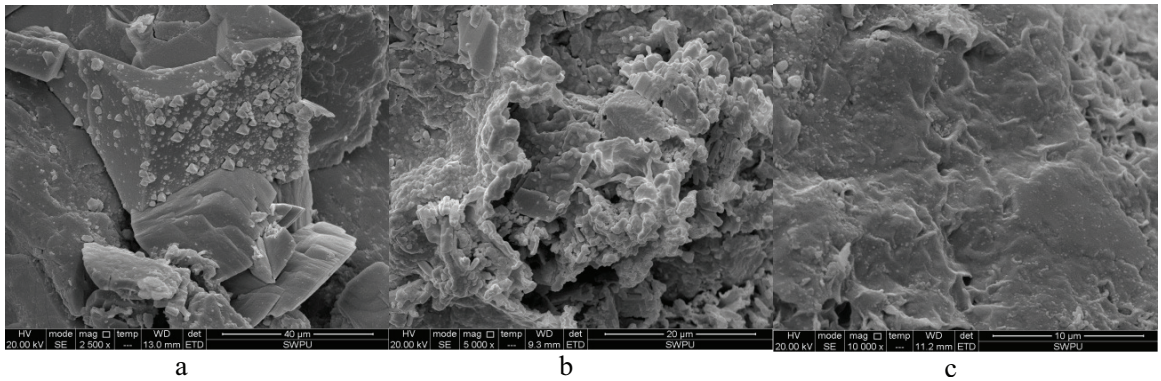

Fig. 6. SEM micrographs of the front end of number 6 core after displacement experiments.

Acknowledgements

This study was funded by the National Special Science & Technology Projects of China during the 13th Five-year Plan (no. 2016ZX05058-003-020).

References

[1] T.S. Mykkeltvedt, X. Raynaud, K.A. Lie, Fully implicit higher-order schemes applied to polymer flooding, Comput. Geosci., 21 (2017) 1245–1266.
[2] X. Kang, J. Zhang, F. Sun, F. Zhang, G. Feng, J. Yang, X. Zhang, W. Xiang, A review of polymer EOR on offshore heavy oil field in Bohai Bay, China. SPE Enhanced Oil Recovery Conference; Kuala Lumpur, Malaysia: Society of Petroleum Engineers (2011).
[3] H. Chen, X. Zhang, Y. Chen, H. Tang, Y. Mei, B. Li, X. Shen, Study on pressure interval of near-miscible flooding by production gas Re-injection in QHD offshore oilfield, J. Petrol. Sci. Eng., 157 (2017) 340–348.
[4] H.X. Chen, H.M. Tang, X.P. Gong, J.J. Wang, Y.G. Liu, M. Duan, F. Zhao, Effect of partially hydrolyzed polyacrylamide on emulsification stability of wastewater produced from polymer flooding, J. Petrol. Sci. Eng., 133 (2015) 431–439.
[5] H.X. Chen, H.M. Tang, M. Duan, Y.G. Liu, M. Liu, F. Zhao, Oil–water separation property of polymer-contained wastewater from polymer-flooding oilfields in Bohai Bay, China, Environ. Technol., 36 (2015) 1373–1380.
[6] Y. Liu, H. Tang, H. Chen, Y. Li, S. Wang, J. Gao, Study on produced water quality variation rule from polymer flooding and mechanism of formation damage, Offshore Oil, 30 (2010) 86–91 (in Chinese).
[7] J.J. Sheng, Formation damage in chemical enhanced oil recovery processes, Asia-Pac. J. Chem. Eng., 11 (2016) 826–835.
[8] H. Hoteit, D. Alexis, O.O. Adepoju, A. Chawathe, T. Malik, Numerical and experimental investigation of polymer-induced resistance to flow in reservoirs undergoing a chemical flood. In SPE Annual Technical Conference and Exhibition. Society of Petroleum Engineers (2016, September).
[9] M. Shoaib, Adsorption of EOR Polymers and Surfactants on Carbonate Minerals, Master's thesis, University of Waterloo (2014).
[10] Z.H. Liu, C.C. Zhou, L.H. Zhang, D.J. Dai, C.L. Li, L. Zhang, G.Q. Liu, Y.J. Shi, An innovative method to evaluate formation pore structure using NMR logging data. In 48th Annual Logging Symposium. Society of Petrophysicists and Well-Log Analysts, 2007.
[11] G. Layrac, C. Gerardin, D. Tichit, S. Harrisson, M. Destarac, Hybrid polyion complex micelles from poly (vinylphosphonic acid)-based double hydrophilic block copolymers and divalent transition metal ions, Polymer, 72 (2015) 292–300.
[12] A. Barhoum, L. Van Lokeren, H. Rahier, A. Dufresne, G. Van Assche, Roles of in situ surface modification in controlling the growth and crystallization of $CaCO_3$ nanoparticles, and their dispersion in polymeric materials, J. Mater. Sci., 50 (2015) 7908–7918.
[13] H. Vehkamäki, Classical nucleation theory in multicomponent systems. Springer, Berlin Heidelberg, 2006.
[14] S. Weiner, L. Addadi, Crystallization pathways in biomineralization, Annu. Rev. mater. Res., 41 (2011) 21–40.
[15] F. Manoli, S. Koutsopoulos, E. Dalas, Crystallization of calcite on chitin, J. Crystal Growth, 182 (1997) 116–124.
[16] K. Naka, S.C. Huang, Y. Chujo, Formation of stable vaterite with poly (acrylic acid) by the delayed addition method, Langmuir, 22 (2006) 7760–7767.
[17] Y.Y. Wang, Q.Z. Yao, H. Li, G.T. Zhou, Y.M. Sheng, Formation of vaterite mesocrystals in biomineral-like structures and implication for biomineralization, Crystal Growth Design, 15 (2015) 1714–1725.
[18] Y. Boyjoo, V.K. Pareek, J. Liu, Synthesis of micro and nano-sized calcium carbonate particles and their applications, J. Mater. Chem., A 2 (2014) 14270–14288.
[19] S. Ouyang, W. Sun, H. Huang, Multi-method synergistic characterization of total pore structure of extra-low permeability sandstone reservoirs: case study of the Heshui area of Ordos Basin, Petrol. Geol. Experim., 40 (2018) 595–604.